B Decays at BABAR

J.J.Back[a*]

[a]Physics Department, Queen Mary, University of London,
Mile End Road, London, E1 4NS, UK (on behalf of the BABAR Collaboration)

We present branching fraction and CP asymmetry results for a variety of B decays based on up to 56.4 fb^{-1} collected by the BABAR experiment running near the $\Upsilon(4S)$ resonance at the PEP-II e^+e^- B-factory.

1. The BABAR Detector

The results presented in this paper are based on an integrated luminosity of up to 56.4 fb^{-1} collected at the $\Upsilon(4S)$ resonance with the BABAR detector [1] at the PEP-II asymmetric e^+e^- collider at the Stanford Linear Accelerator Center. Charged particle track parameters are measured by a five-layer double-sided silicon vertex tracker and a 40-layer drift chamber located in a 1.5-T magnetic field. Charged particle identification is achieved with an internally reflecting ring imaging Cherenkov detector (DIRC) and from the average dE/dx energy loss measured in the tracking devices. Photons and π^0s are detected with an electromagnetic calorimeter (EMC) consisting of 6580 CsI(Tl) crystals. An instrumented flux return (IFR), containing multiple layers of resistive plate chambers, provides muon and long-lived hadron identification.

2. B Decay Reconstruction

The B meson candidates are identified kinematically using two independent variables. The first is $\Delta E = E^* - E^*_{beam}$, which is peaked at zero for signal events, since the energy of the B candidate in the $\Upsilon(4S)$ rest frame, E^*, must be equal to the energy of the beam, E^*_{beam}, by energy conservation. The second is the beam-energy substituted mass, $m_{\mathrm{ES}} = \sqrt{(E^{*2}_{beam} - \mathbf{p}^{*2}_B)}$, where $\mathbf{p}^*_B$ is the momentum of the B meson in the $\Upsilon(4S)$ rest frame, and must be close to the nominal B mass [5]. The resolution of m_{ES} is dominated by the beam energy spread and is approximately 2.5 MeV/c^2.

Several of the B modes presented here have decays that involve neutral pions (π^0) and K^0_s particles. Neutral pion candidates are formed by combining pairs of photons in the EMC, with requirements made to the energies of the photons and the mass and energy of the π^0. Table 1 shows these requirements for various decay modes, as well as the selection requirements for K^0_s candidates, which are made by combining oppositely charged pions.

Significant backgrounds from light quark-antiquark continuum events are suppressed using various event shape variables which exploit the difference in the event topologies in the centre-of-mass frame between background events, which have a di-jet structure, and signal events, which tend to be rather spherical. One example is the cosine of the angle θ^*_T between the thrust axis of the signal B candidate and the thrust axis of the rest of the tracks and neutrals in the event. This variable is strongly peaked at unity for continuum backgrounds and is flat for signal.

Further suppression of backgrounds can be achieved using a Fisher discriminant $\mathcal{F}$, which is a linear combination of event shape variables, such as the scalar sum of the centre-of-mass momenta of all charged tracks and neutrals, excluding the B decay products, flowing into nine concentric cones centred on the thrust axis of the B candidate. Signal events have a lower Fisher discriminant value compared to background events, as shown in Fig. 1.

Sidebands in on-resonance ($\Upsilon(4S)$) data are

Table 1
Selection requirements for π^0 and K_S^0 candidates for various B decay modes ($h = K/\pi$). E_γ is the minimum photon energy and m_{π^0} and E_{π^0} the mass and energy, respectively, of π^0 candidates. The mass of the K_S^0 is $m_{K_S^0}$, the opening angle between the K_S^0 momentum and its line-of-flight is $\phi_{K_S^0}$, the transverse flight distance of the K_S^0 from the primary event vertex is $d_{K_S^0}$ and $\tau/\sigma_{K_S^0}$ is the K_S^0 lifetime divided by its error.

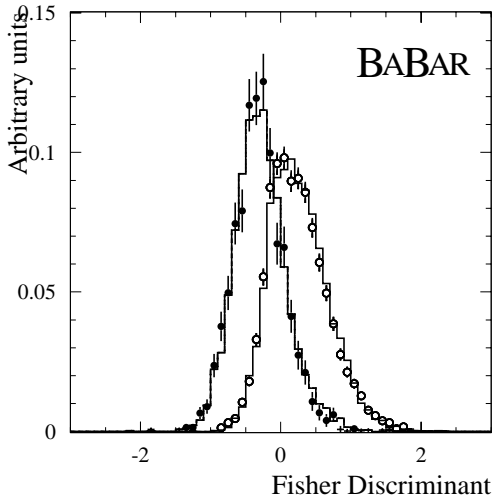| Mode	E_γ (MeV)	m_{π^0} (MeV/c^2)	E_{π^0} (MeV)	$m_{K_S^0}$ (MeV/c^2)	$\phi_{K_S^0}$ (mrad)	$d_{K_S^0}$ (mm)	$\tau/\sigma_{K_S^0}$
$B \to DK$	> 70	[124, 144]	> 200	—	—	—	—
$B \to D^{(*)}D^{(*)}$	> 30	[115, 155]	> 200	[473, 523]	< 200	> 2	—
$B \to h\pi^0$	> 30	[111, 159]	—	—	—	—	—
$B \to hK^0$	—	—	—	[487, 509]	—	—	> 5
$B \to \phi K^{(*)}$	—	—	—	[487, 510]	< 100	—	> 3
$B \to \eta h$	> 50	[120, 150]	—	—	—	—	—
$B \to \eta K^0$	> 50	[115, 155]	—	[491, 507]	< 40	> 2	—
$B \to \eta' K^{(*)0}$	—	—	—	[488, 508]	—	—	—
$B \to K^*\gamma$	> 30	[115, 150]	> 200	[489, 507]	—	—	—
$B \to K^{(*)}\ell^+\ell^-$	—	—	—	[480, 498]	—	> 1	—

Figure 1. The Fisher distribution for $B^0 \to \pi^+\pi^-$ signal Monte Carlo simulated events (left histogram) compared to data $B^- \to D^0\pi^-$ decays (black points), and continuum background Monte Carlo (right histogram) compared to on-resonance sideband data (open points).

used to characterise the light quark background in ΔE and $m_{\rm ES}$, as well as data taken at 40 MeV below the $\Upsilon(4S)$ resonance ("off-resonance"). The phenomenologically motivated Argus function [2] is used to fit the background $m_{\rm ES}$ distributions. Control samples are used to compare the performance between Monte Carlo simulated events and on-resonance data.

The results presented here are from either extended maximum likelihood fits or from cut-and-count methods. All of the analyses have been performed "blind", meaning that the signal region is looked at only after the selection criteria have been finalised (in order to reduce the risk of bias).

Charge conjugate modes are implied throughout this paper.

3. $B \to DK$

The decays $B^- \to D^0K^-$ and $B^\pm \to D_\pm^0 K^\pm$, where $D_\pm^0$ denotes the CP-even (+) or CP-odd states ($-$) $(D^0 \pm \bar{D}^0)/\sqrt{2}$, can be used to measure in a theoretically clean way the Cabibbo-Kobayashi-Maskawa (CKM) angle γ, one of the parameters that describes CP Violation in the Standard Model [3] [4]. Figure 2 shows a graphical representation of the relation between the amplitudes of the decays and the angle γ.

This measurement is experimentally challenging because the branching fractions of these decays are of the order of 10^{-7}. However, in the meantime we can measure the ratio between the
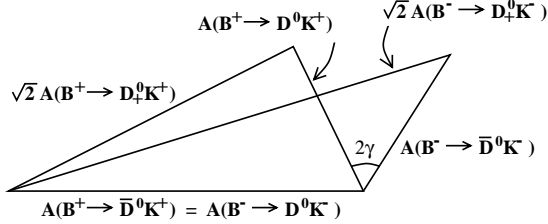
Figure 2. Relation between the amplitudes for the processes $B \to DK$ and the angle γ.

branching fractions for $B^- \to D^0 K^-$ and $B^- \to D^0 \pi^-$, where the final states for the D^0 meson are $K^- \pi^+$, $K^- \pi^+ \pi^- \pi^+$ and $K^- \pi^+ \pi^0$. The invariant masses of $D^0 \to K^- \pi^+, K^- \pi^+ \pi^- \pi^+$ candidates are required to be within 20.4 MeV/c^2 (3 σ) of the nominal value [5]. Since the mode $D^0 \to K^- \pi^+ \pi^0$ has more combinatorial background compared to the other decays, the invariant mass is required to be within two standard deviations (2×11 MeV/c^2).

Three event shape variables are used to suppress light-quark continuum background events. The first is the normalised Fox-Wolfram moment H_2/H_0 [6], which is required to be less than 0.5 for all selected events. The second variable is θ_T^*, mentioned in section 2. The value of $|\cos\theta_T^*|$ is required to be less than 0.9 for the $D^0 \to K^+ \pi^-$ mode and less than 0.7 for $D^0 \to K^- \pi^+ \pi^- \pi^+$ and $D^0 \to K^- \pi^+ \pi^0$. Thirdly, we use the helicity angle θ_{hel}, defined as the angle between the direction of the D^0 candidate calculated in the rest frame of the B and the direction of one of the decay products of the D^0, calculated in the rest frame of the D^0. The distribution of $\cos\theta_{hel}$ is flat for signal and peaked at ±1 for fake D^0 events. For continuum events, $|\cos\theta_T^*|$ and $\cos\theta_{hel}$ are correlated, and we use

$$|\cos\theta_{hel}| < 0.9; \quad 0.0 \le |\cos\theta_T^*| < 0.7$$
$$|\cos\theta_{hel}| < -3|\cos\theta_T^*| + 3; \quad 0.7 \le |\cos\theta_T^*| \le 1.0. \tag{1}$$

The yields for the signal modes are found by using an unbinned extended maximum likelihood fit to the ΔE and $m_{\rm ES}$ variables, together with the Cherenkov angles (θ_C) of the prompt tracks measured by the DIRC (to distinguish kaons from pions). We obtain

$$
\begin{aligned}
R &= \frac{\mathcal{B}(B^- \to D^0 K^-)}{\mathcal{B}(B^- \to D^0 \pi^-)} \\
&= (8.31 \pm 0.35 \pm 0.13)\%, \tag{2}
\end{aligned}
$$

where the first error is statistical and the second error is systematic. This quantity has also been measured by the CLEO and BELLE Collaborations, where they get $R = (5.5 \pm 1.4 \pm 0.5)\%$ [7] and $R = (7.9 \pm 0.9 \pm 0.6)\%$ [8], respectively. Theory predicts, using factorisation and tree-level Feynman diagrams only, a value $R \approx \tan^2\theta_C (f_K/f_\pi)^2 \approx 7.4\%$, where θ_C is the Cabibbo angle, and f_K and f_π are the meson decay constants. For the CP-even mode $D_+^0 \to K^+ K^-$ we have measured

$$
\begin{aligned}
R_{CP} &= \frac{\mathcal{B}(B^- \to D_+^0 K^-) + \mathcal{B}(B^+ \to D_+^0 K^+)}{\mathcal{B}(B^- \to D_+^0 \pi^-) + \mathcal{B}(B^+ \to D_+^0 \pi^+)} \\
&= (8.4 \pm 2.0 \pm 0.8)\%, \tag{3}
\end{aligned}
$$

and the direct CP asymmetry

$$
\begin{aligned}
\mathcal{A}_{CP} &= \frac{\mathcal{B}(B^- \to D_+^0 K^-) - \mathcal{B}(B^+ \to D_+^0 K^+)}{\mathcal{B}(B^- \to D_+^0 K^-) + \mathcal{B}(B^+ \to D_+^0 K^+)} \\
&= 0.15 \pm 0.24^{+0.07}_{-0.08}. \tag{4}
\end{aligned}
$$

4. $B \to D^{(*)} D^{(*)}$

Time-dependent CP violating asymmetries in the decays $B \to D^{(*)} D^{(*)}$ can be used to measure the CKM angle β [9], in a way complimentary to measurements already made with decays such as $B^0 \to J/\psi K_S^0$ [10]. However, the vector-vector decay of $B^0 \to D^{*+} D^{*-}$ is not a pure CP eigenstate, which may cause a sizeable dilution to the CP violation that can be observed. In principle, a full time-dependent angular analysis can remove this dilution [11].

We reconstruct exclusively the decays $B^0 \to D^{*+} D^{*-}$ and $B^0 \to D^{*\pm} D^\mp$, where $D^{*\pm} \to D^0 \pi^\pm$ or $D^\pm \pi^0$. The final states we consider for the neutral D mesons are $K^- \pi^+$, $K^- \pi^+ \pi^0$, $K^- \pi^+ \pi^- \pi^+$ and $K_S^0 \pi^+ \pi^-$, while we consider the D^+ final states $K^- \pi^+ \pi^+$, $K_S^0 \pi^+$ and $K^- K^+ \pi^+$.

B^0 candidates are reconstructed by performing a mass-constrained fit to the D and D^* candidates. In the case when more than one B candidate is found for an event, we chose the B candidate in which the D and D^* mesons have invariant masses closest to their nominal values [5].

Signal events are required to satisfy $|\Delta E| < 25$ MeV and $5.273 < m_{ES} < 5.285$ GeV/c^2.

Using a sample of 22.7 million $B\overline{B}$ pairs, we obtain the following branching fractions

$$\mathcal{B}(B^0 \to D^{*+}D^{*-}) = (8.0 \pm 1.6 \pm 1.2) \times 10^{-4}, \quad (5)$$

$$\mathcal{B}(B^0 \to D^{*\pm}D^{\mp}) = (6.7^{+2.0}_{-1.7} \pm 1.1) \times 10^{-4}. \quad (6)$$

The fraction of the CP-odd component R_t of $B^0 \to D^{*+}D^{*-}$ decays can be found by using the angular distribution of the decay in the transversity basis [11]

$$\frac{1}{\Gamma}\frac{d\Gamma}{d\cos\theta_{tr}} = \frac{3}{4}(1 - R_t)\sin^2\theta_{tr} + \frac{3}{2}R_t\cos^2\theta_{tr}, \quad (7)$$

where Γ is the decay rate and θ_{tr} is the polar angle between the normal to the D^{*-} decay plane and the π^+ line of flight in the D^{*+} rest frame. Using an unbinned extended maximum likelihood fit, we find

$$R_t = 0.22 \pm 0.18 \pm 0.03. \quad (8)$$

5. Two-body Charmless B Decays

Measurements of the branching fractions and CP asymmetries for B decays into two-body charmless final states will give us important information about the CKM angles α and γ [12]. The time-dependent CP-violating asymmetry in the decay $B^0 \to \pi^-\pi^+$ is related to the angle α. If the decay proceeds only through tree diagrams, then the asymmetry is directly related to α. However, we can only measure an effective angle, α_{eff}, if there is pollution from gluonic penguins. In principle, α can be extracted by using the isospin-related decays $B^+ \to \pi^+\pi^0$ and $B^0 \to \pi^0\pi^0$ [13]. It is also possible to get a bound on the value of α [14] via

$$\sin^2(\alpha_{eff} - \alpha) < \frac{\langle\mathcal{B}(B^0 \to \pi^0\pi^0)\rangle_{CP}}{\mathcal{B}(B^+ \to \pi^+\pi^0)}, \quad (9)$$

where $\langle\mathcal{B}(B^0 \to \pi^0\pi^0)\rangle_{CP} = \frac{1}{2}[\mathcal{B}(B^0 \to \pi^0\pi^0) + \mathcal{B}(\bar{B}^0 \to \pi^0\pi^0)]$. The angle γ can be constrained by using ratios of branching fractions for various $\pi\pi$ and $K\pi$ decays [15].

Here, we consider only decays involving at least one neutral particle in the final state (see [16] for results on $B^0 \to h^+h^-$ decays, where $h = \pi$ or K).

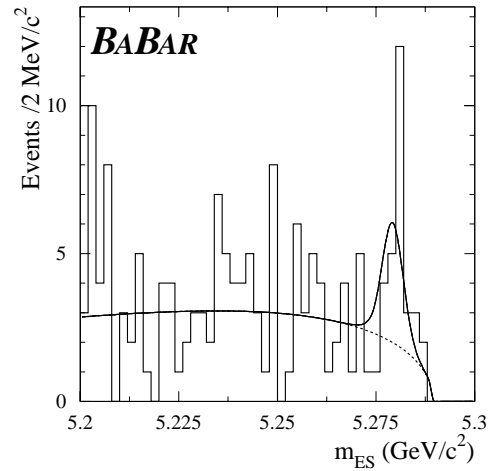

Figure 3. Distribution of m_{ES} for $B^+ \to \pi^+\pi^0$ events in on-resonance data. The solid curve represents the projection of the maximum likelihood fit result, while the dotted curve represents the background contribution.

Backgrounds from non-hadronic events are reduced by requiring H_2/H_0 [6] to be less than 0.95 and the sphericity [17] of the event to be greater than 0.01. Light-quark continuum events are suppressed by using two other event shape variables. The first is the angle θ_S^* in the centre-of-mass frame between the sphericity axis of the B candidate and of the remaining tracks and neutrals in the event. The distribution of $|\cos\theta_S^*|$ is peaked near unity for background and is approximately uniform for signal events. We require $|\cos\theta_S|$ to

be less than 0.9 for hK_s^0, 0.8 for $h\pi^0$ and 0.7 for $\pi^0\pi^0$.

The second variable is the Fisher discriminant $\mathcal{F}$ mentioned in section 2.

The branching fractions and charge asymmetries shown in Table 2 are obtained from an unbinned extended maximum likelihood fit using $\mathcal{F}$, θ_C, m_{ES} and ΔE. Figure 3 shows the m_{ES} distribution for $B^+ \rightarrow \pi^+\pi^0$ decays, in which we observe a signal for the first time.

Table 2

Two-body charmless B decay branching fractions ($\mathcal{B}$) and CP asymmetries ($\mathcal{A}_{CP}$) based on 56.4 fb^{-1}. Upper limits are given at the 90% confidence level.

Mode	$\mathcal{B}$ (10^{-6})	$\mathcal{A}_{CP}$
$\pi^+\pi^0$	$4.1^{+1.1+0.8}_{-1.0-0.7}$	$-0.02^{+0.27}_{-0.26} \pm 0.10$
$K^+\pi^0$	$11.1^{+1.3}_{-1.2} \pm 1.0$	$0.00 \pm 0.11 \pm 0.02$
π^+K^0	$17.5^{+1.8}_{-1.7} \pm 1.8$	$-0.17 \pm 0.10 \pm 0.02$
$K^+\overline{K}^0$	$< 1.4(-0.6^{+0.6}_{-0.7} \pm 0.3)$	—
$\pi^0\pi^0$	$< 3.4(-0.9^{+0.9+0.8}_{-0.7-0.6})$	—

6. Three-body Charmless Charged B Decays

The decays $B^+ \rightarrow h^+h^-h^+$, where $h = \pi$ or K, can be used to measure the angle γ [18]. The basic idea is that there can be interference between resonant and non-resonant amplitudes leading to direct CP violation. A Dalitz plot analysis can, in principle, give us information about all of the strong and weak phases in these decays. A first step towards this goal is to measure the branching fractions into the whole Dalitz plot. We can write these as

$$\mathcal{B} = \frac{1}{N_{B\overline{B}}} \sum_i \frac{S_i}{\epsilon_i}, \qquad (10)$$

where $N_{B\overline{B}}$ is the total number of $B\overline{B}$ pairs in the data sample, S_i is the net signal (after background subtraction) in cell i of the Dalitz plot and ϵ_i is the signal efficiency in that cell found from Monte Carlo simulation. No assumptions are made about intermediate resonances.

B candidates are formed by combining three charged tracks. We use dE/dx information from the tracking devices and the Cherenkov angle and number of photons measured by the DIRC for tracks with momenta above 700 MeV/c, to identify charged pions and kaons. Electron candidates are vetoed by requiring that they fail a selection based on information from dE/dx, shower shapes in the EMC and the ratio of the shower energy and track momentum. We remove B candidates when the combination of any two of its (oppositely charged) daughter tracks is within 3 σ of the mass of the D^0, J/ψ or $\psi(2S)$ mesons. Here, σ is 10.0 MeV/c^2 for D^0 and 15.0 MeV/c^2 for J/ψ and $\psi(2S)$.

Continuum backgrounds are suppressed by requiring selections on $|\cos\theta_T^*|$ and on the Fisher discriminant mentioned in section 2. Comparisons between Monte Carlo simulated events and on-resonance data are made using the control sample $B^- \rightarrow D^0(\rightarrow K^-\pi^+)\pi^-$, which has a similar decay topology as the charmless signal modes.

The signal region is defined as $|m_{ES} - m_B| <$ 8.0 MeV/c^2 and $|\Delta E - \langle\Delta E\rangle| <$ 60.0 MeV, where $\langle\Delta E\rangle$ is 7.0 MeV (obtained from the $D^0\pi^-$ control sample) and m_B is the nominal mass of the charged B meson [5].

Table 3 shows the results for 51.5 fb^{-1}, where we have also included the results from the BELLE Collaboration [19] for comparison. Figure 4 shows preliminary unbinned Dalitz plots for $B^+ \rightarrow K^+\pi^-\pi^+$ and $B^+ \rightarrow K^+K^-K^+$ in on-resonance data (with no background subtraction or efficiency corrections applied). As a cross-check, we measure $(180 \pm 4 \pm 11) \times 10^{-6}$ for the branching fraction for the $B^- \rightarrow D^0\pi^-$ control sample, which agrees with the previously measured value of $(203 \pm 20) \times 10^{-6}$ [5].

7. $B \rightarrow \phi K^{(*)}, \phi\pi$

These modes are interesting because only penguin diagrams contribute to the decay amplitudes (mainly $b \rightarrow s\bar{s}s$), and the time-dependent CP asymmetry for the neutral mode $B^0 \rightarrow \phi K_s^0$ can be used to measure $\sin 2\beta$. Comparison with $\sin 2\beta$ results from charmonium modes will allow us to probe new physics participating in pen-
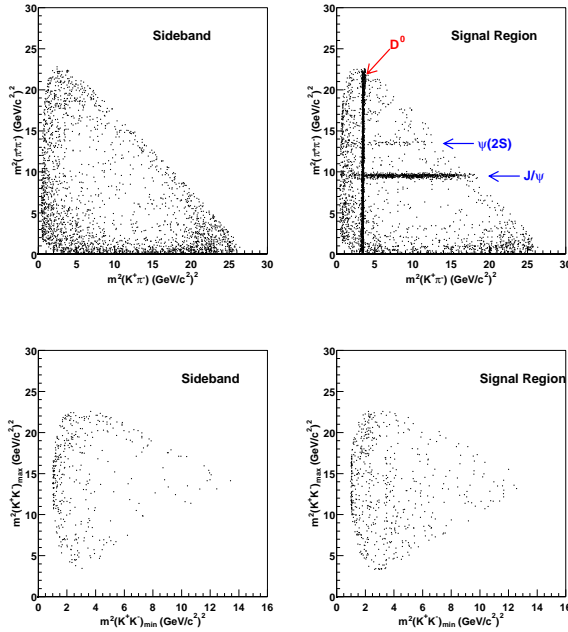
Figure 4. Unbinned Dalitz plots (with no background subtraction or efficiency corrections) for $B^+ \to K^+\pi^-\pi^+$ events in on-resonance sideband (top left) and signal (top right) data, and for $B^+ \to K^+K^-K^+$ events in on-resonance sideband (bottom left) and signal (bottom right) data. Open charm contributions are not removed.

Table 3

Three-body charmless charged B decay branching fractions ($\times 10^{-6}$) from *BABAR* (51.5 fb^{-1}) and BELLE (29.1 fb^{-1}).

Mode	*BABAR*	BELLE
$\pi^+\pi^-\pi^+$	$8.5 \pm 4.0 \pm 3.6 (< 15)$	—
$K^+\pi^-\pi^+$	$59.2 \pm 4.7 \pm 4.9$	$55.6 \pm 5.8 \pm 7.7$
$K^+K^-\pi^+$	$2.1 \pm 2.9 \pm 2.0 (< 7)$	< 21
$K^+K^-K^+$	$34.7 \pm 2.0 \pm 1.8$	$35.3 \pm 3.7 \pm 4.5$

guin loops [9]. Isospin symmetry predicts that

$\mathcal{B}(B^\pm \to \phi K^\pm) \approx \mathcal{B}(B^0 \to \phi K^0)$, and there are theoretical estimates for the various branching fractions based on factorisation models and perturbative QCD [20].

B mesons are reconstructed by combining $\phi \to K^+K^-$ candidates with either a K^* candidate or a bachelor charged track. We consider the decays $K^{*+} \to K^0\pi^+$ (with $K^0_S \to \pi^+\pi^-$), $K^{*+} \to K^+\pi^0$ and $K^{*0} \to K^+\pi^-$.

Continuum backgrounds are suppressed by using a Fisher discriminant and requiring that $|\cos\theta^*_T| < 0.9$.

Table 4 shows the branching fractions for the modes obtained from an extended unbinned maximum likelihood fit using m_{ES}, ΔE, θ_C, the mass of the ϕ resonance, the Fisher discriminant and the cosine of the helicity angle. Also shown in Table 4 are the results from the BELLE [21] and CLEO [22] collaborations.

8. Charmless B decays with η and η' mesons

These rare decays proceed via $b \to u$ tree and $b \to s$ penguin Feynman diagrams. Interference between the various amplitudes can give rise to direct CP violation and the time-dependent CP asymmetries for the neutral modes are sensitive to the value of $\sin 2\beta$. The CLEO collaboration has observed unexpectedly high branching fractions for $B \to \eta K^*$ and $B \to \eta' K$ [23], leading some theorists to speculate on exotic processes such as QCD anomalies and penguins with an enhanced charm contribution in the virtual loop [24].

We have studied the decays $B \to \eta h, \eta K^*, \eta' K$ and $\eta' K^{*0}$. The η resonances are formed by combining two photons, each with a minimum energy of 50 MeV, while η' mesons are reconstructed in the final states $\eta' \to \eta\pi^+\pi^-$ or $\eta' \to \rho^0\gamma$, where $\rho^0 \to \pi^+\pi^-$. The ρ^0 candidates are required to have an invariant mass between 500 and 995 MeV/c^2. We consider the same neutral and charged K^* decays as those in the $B \to \phi K^*$ analysis mentioned in section 7.

Like other analyses, the requirement $|\cos\theta^*_T| < 0.9$ is imposed to suppress continuum background.

Table 4
Branching fractions ($\times 10^{-6}$) for $B \to \phi K$ and $B^+ \to \phi \pi^+$ decays from *BABAR* (56.3 fb^{-1} and 20.7 fb^{-1}†),
BELLE (21.6 fb^{-1}) and CLEO (9.1 fb^{-1}).

Mode	*BABAR*	BELLE	CLEO
ϕK^+	$9.2 \pm 1.0 \pm 0.8$	$11.2^{+2.2}_{-2.0} \pm 1.4$	$5.5^{+2.1}_{-1.8} \pm 0.6$
ϕK^0	$8.7^{+1.7}_{-1.5} \pm 0.9$	$8.9^{+3.4}_{-2.7} \pm 1.0$	< 12.3
ϕK^{*+}	$9.7^{+4.2}_{-3.4} \pm 1.7$†	< 36	< 22.5
ϕK^{*0}	$8.7^{+2.5}_{-2.1} \pm 1.1$†	$13.0^{+6.4}_{-5.2} \pm 2.1$	$11.5^{+4.5+1.8}_{-3.7-1.7}$
$\phi \pi^+$	< 0.6	—	< 5

We use the energy constrained mass m_{EC}, which is the mass of the B candidate when its energy is constrained to be equal to the beam energy, instead of $m_{\rm ES}$.

Table 5 shows the branching fraction results from *BABAR* using extended unbinned maximum likelihood fits to the data. The main variables in the fits are m_{EC}, ΔE, the invariant mass and helicity distributions of the intermediate resonance and a Fisher discriminant. Also shown are the results from CLEO [23] and BELLE. We confirm the large branching fractions for the ηK^* and $\eta' K$ modes.

9. $B \to K^* \gamma$

The exclusive decays $B \to K^* \gamma$ proceed via the flavour-changing neutral $b \to s\gamma$ transition, where the largest contribution comes from the top quark in the electromagnetic penguin virtual loop. The current Standard Model next-to-leading order predictions for the branching fractions for these modes lies between 3.5×10^{-4} and 6.2×10^{-4} [25]. New physics contributions may enhance the observed branching fractions.

The decays $B^0 \to K^{*0} \gamma$ and $B^+ \to K^{*+} \gamma$ have been studied. The K^* is formed by combining K^+, K_S^0, π^- and π^0 candidates through the four decay modes $K^{*0} \to K^+ \pi^-, K_S^0 \pi^0$ and $K^{*+} \to K^+ \pi^0, K_S^0 \pi^+$.

The background from these decays is predominantly from light-quark continuum events, and are suppressed by requiring selections on $|\cos \theta_T^*|$ and the helicity angle. The branching fractions are found by using an unbinned maximum likelihood fit to the $m_{\rm ES}$ distributions, with the re-

Table 6
Branching fraction ($\mathcal{B}$) and CP asymmetry ($\mathcal{A}_{CP}$) results for the $B \to K^* \gamma$ channels for 20.7 fb^{-1}.

Mode	$\mathcal{B}(\times 10^{-5})$	$\mathcal{A}_{CP}$
$B^0 \to K^{*0} \gamma$	$4.23 \pm 0.40 \pm 0.22$	$-0.05 \pm 0.09 \pm 0.01$
$B^+ \to K^{*+} \gamma$	$3.83 \pm 0.62 \pm 0.22$	$-0.04 \pm 0.13 \pm 0.01$

quirements $-200 < \Delta E < 100$ MeV for the $K^+ \pi^-$ and $K_S^0 \pi^+$ modes and $-225 < \Delta E < 125$ MeV for the modes containing a π^0 ($K^+ \pi^0$ and $K_S^0 \pi^0$). Table 6 shows the branching fraction and CP asymmetry results for 20.7 fb^{-1}, where the CP asymmetry for these decays is defined as

$$\mathcal{A}_{CP} = \frac{\mathcal{B}(\bar{B} \to \bar{K}^* \gamma) - \mathcal{B}(B \to K^* \gamma)}{\mathcal{B}(\bar{B} \to \bar{K}^* \gamma) + \mathcal{B}(B \to K^* \gamma)}. \quad (11)$$

Theoretical expectations for the branching fractions are in agreement with the measured values.

10. $B \to K^{(*)} \ell^+ \ell^-$

The decays $B \to K^{(*)} \ell^+ \ell^-$, where $\ell^\pm$ is a charged lepton, proceed via flavour-changing neutral currents, which are highly suppressed in the Standard Model. The dominant contributions come from one-loop electroweak penguins, with branching fractions predicted at the $10^{-7} - 10^{-6}$ level [26]. These could be enhanced if new, heavy particles, such as those from supersymmetric models, appear in the virtual loop.

We consider the four decay modes $B^+ \to K^+ \ell^+ \ell^-$, $B^0 \to K_S^0 \ell^+ \ell^-$, $B^+ \to K^{*+} \ell^+ \ell^-$ and $B^0 \to K^{*0} \ell^+ \ell^-$, where $K^{*0} \to K^+ \pi^-$, $K^{*+} \to K_S^0 \pi^+$, $K_S^0 \to \pi^+ \pi^-$, and ℓ is either an e or

Table 5
Measured branching fractions ($\times 10^{-6}$) for B decays with η and η' mesons from the CLEO, BELLE and *BABAR* collaborations.

Mode	CLEO ($9.1\,\mathrm{fb}^{-1}$)	BELLE ($29\,\mathrm{fb}^{-1}$)	*BABAR* ($56\,\mathrm{fb}^{-1}$, $21\,\mathrm{fb}^{-1}$†)
$\eta\pi^+$	$1.2^{+2.8}_{-1.2}(< 5.7)$	$5.4^{+2.0}_{-1.7} \pm 0.6$	$2.2^{+1.8}_{-1.6} \pm 0.1(< 5.2)$†
ηK^+	$2.2^{+2.8}_{-2.2}(< 6.9)$	$5.3^{+1.8}_{-1.5} \pm 0.6$	$3.8^{+1.8}_{-1.5} \pm 0.2(< 6.4)$†
ηK^0	$0.0^{+3.2}_{-0.0}(< 9.3)$		$6.0^{+3.8}_{-2.9} \pm 0.4(< 12)$†
ηK^{*0}	$13.8^{+5.5}_{-4.6} \pm 1.6$	$16.5^{+4.6}_{-4.2} \pm 1.2$	$19.8^{+6.5}_{-5.6} \pm 1.5$†
ηK^{*+}	$26.4^{+9.6}_{-8.2} \pm 3.3$	$26.5^{+7.8}_{-7.0} \pm 3.0$	$22.1^{+11.1}_{-9.2} \pm 3.2$†
$\eta' K^+$	$80^{+10}_{-9} \pm 7$	$78 \pm 6 \pm 9$	$67 \pm 5 \pm 5$
$\eta' K^0$	$89^{+18}_{-16} \pm 9$	68 ± 10	$46 \pm 6 \pm 4$
$\eta' K^{*0}$	$7.8^{+7.7}_{-5.7}(< 24)$		$4.0^{+3.5}_{-2.4} \pm 1.0(< 13)$

μ. We require the two oppositely charged leptons to each have a momentum greater than 0.5 (1.0) GeV for $e(\mu)$. Electron-positron pairs consistent with photon conversions are removed from the data sample. K^* candidates are required to have an invariant mass within 75 MeV/c^2 of the mean mass of 892 MeV/c^2 [5]. The charm decays $B \to J/\psi(\ell^+\ell^-)K^{(*)}$ and $B \to \psi(2S)(\ell^+\ell^-)K^{(*)}$ have identical topologies to signal events, and are suppressed by applying a veto in the ΔE versus invariant mass of the lepton pair ($m_{\ell^+\ell^-}$) plane, as shown in Fig. 5. The signal is extracted using a two-dimensional extended unbinned maximum likelihood fit to m_{ES} and ΔE in the region $m_{\mathrm{ES}} > 5.2$ GeV/c^2 and $|\Delta E| < 0.25$ GeV. For an integrated luminosity of 56.4 fb^{-1}, we obtain the preliminary branching fractions

$$\mathcal{B}(B^0 \to K\ell^+\ell^-) = 8.4^{+3.0+1.0}_{-2.4-1.8} \times 10^{-7}, \qquad (12)$$

$$\mathcal{B}(B^0 \to K^*\ell^+\ell^-) < 35 \times 10^{-7}(90\% C.L.), \quad (13)$$

where the first result represents an observation at the 5 sigma level (statistical errors only). Figure 6 shows the projections from the likelihood fits onto m_{ES} for the signal region in ΔE.

11. Conclusions

We have shown a selection of results from the *BABAR* experiment based on up to 56.4 fb^{-1} collected at the $\Upsilon(4S)$ resonance. We have made the following observations:
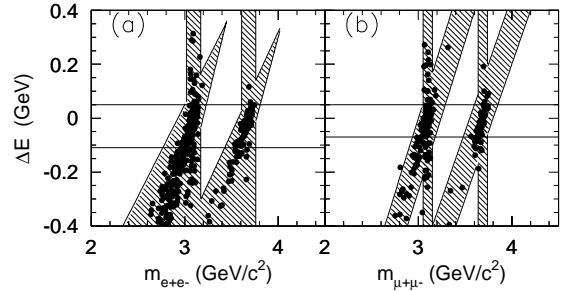

Figure 5. Veto in the ΔE vs.$m_{\ell^+\ell^-}$ plane for (a) $B \to K^{(*)}e^+e^-$ and (b) $B \to K^{(*)}\mu^+\mu^-$. The hatched regions are vetoed. The dots correspond to $B \to J/\psi(\ell^+\ell^-)K$ and $B \to \psi(2S)(\ell^+\ell^-)K$ Monte Carlo simulated events, while the horizontal lines show the boundaries for the ΔE region where most of the signal events would lie.

- $B \to DK$. We have measured the ratio of the branching fractions for $B^- \to D^0 K^-$ and $B^- \to D^0\pi^-$, as well as the *CP* asymmetry for the *CP*-even mode $B^- \to D^0_+ K^-$, which is the first step towards measuring γ.

- $B \to D^{(*)}D^{(*)}$ decays, which can be used to measure β, have been fully reconstructed. We have a first measurement of the *CP*-odd content of these decays.
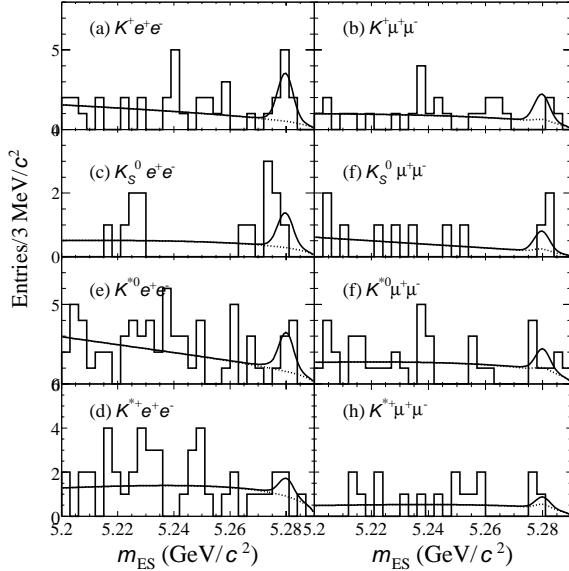
Figure 6. Projections from the likelihood fits of the $K^{(*)}\ell^+\ell^-$ modes onto $m_{\rm ES}$ for the signal region $-0.11 < \Delta E < 0.05$ GeV for electrons and $-0.07 < \Delta E < 0.05$ GeV for muons. The dotted lines show the level of background, while the solid lines show the sum of the signal and background contributions.

- We observe $B^+ \rightarrow \pi^+\pi^0$ for the first time, which, with other two body charmless modes, can be used to extract the angle α.

- Three-body charmless B decays. Significant signals have been observed for $B^+ \rightarrow K^+\pi^-\pi^+$ and $B^+ \rightarrow K^+K^-K^+$. A Dalitz plot analysis of these decays could give us information about the angle γ.

- We have made observations of the decays $B^+ \rightarrow \phi K^+$ and $B^0 \rightarrow \phi K^0$, and we also confirm the rather large branching fractions of ηK^* and $\eta' K$ first seen by CLEO, which presents a theoretical challenge.

- Radiative penguin modes. We observe a signal for $B^0 \rightarrow K\ell^+\ell^-$ for the first time.

Many of the results are approaching the level of predictions from the Standard Model. We observe no direct CP violation in several decays, which could indicate that (the differences between) strong phases are small. We can expect many more fruitful searches and improvements to existing measurements in the near future.

REFERENCES

1. *BABAR* Collaboration, B. Aubert *et al.,* "The *BABAR* Detector", Nucl. Instr. and Meth. A **479**, 1 (2002), hep-ex/0105044.
2. ARGUS Collaboration, H. Albrecht *et al.,*Z. Phys. C **48**, 543 (1990).
3. M. Gronau and D. Wyler, Phys. Lett. B **265**, 172 (1991); M. Gronau and D. London, Phys. Lett. B **253**, 483 (1991).
4. D. Atwood, I. Dunietz and A. Soni, Phys. Rev. Lett. **78**, 3257 (1997).
5. Particle Data group, D. E. Groom *et al.,*, Eur. Phys. Jour. C **15**, 1 (2000).
6. G. C. Fox and S. Wolfram, Phys. Rev. Lett. **41**, 1581 (1978).
7. M. Athanas *et al.,* Phys. Rev. Lett. **80**, 5493 (1998), hep-ex/9802023.
8. BELLE Collaboration, K. Abe *et al.,* Phys. Rev. Lett. **87**, 111801 (2001), hep-ex/0104051.
9. Y. Grossman and M. Worah, Phys. Lett. B **395**, 241 (1997); R. Fleischer, Int. Jour. Mod. Phys. A **12**, 2459 (1997).
10. *BABAR* Collaboration, B. Aubert *et al.,* SLAC-PUB-9293, hep-ex/0207042 (2002), submitted to Phys. Rev. Lett.
11. I. Dunietz *et al.,* Phys. Rev. D **43**, 2193 (1991).
12. M. Gronau and J. Rosner, Phys. Rev. Lett. **76**, 1200 (1996), hep-ph/9510363; R. Fleischer and T. Mannel, Phys. Lett. B **397**, 269 (1997), hep-ph/9610357;
13. M. Gronau and D. London, Phys. Rev. Lett. **65**, 3381 (1990).

14. Y. Grossman and H. Quinn, Phys. Rev. D **58**, 017504 (1998).

15. M. Neubert, Nucl. Phys. Proc. Suppl. **86**, 477 (2000), hep-ph/9909564.

16. *BABAR* Collaboration, B. Aubert *et al.,* Phys, Rev. Lett. **87**, 151802 (2001), hep-ex/0105061.

17. S. L. Wu, Phys. Rep. **107**, 59 (1984).

18. R. E. Blanco, C. Gobel, R. Mendez-Galain, Phys. Rev. Lett. **86**, 2720 (2001), hep-ph/0007105;
    S. Fajfer, R. J. Oakes, T. N. Pham, Phys. Lett. B **539**, 67 (2002), hep-ph/0203072.

19. BELLE Collaboration, K. Abe *et al.,* Phys. Rev. D **65**, 092005 (2002), hep-ex/0201007.

20. H-Y. Cheng, Talk given at International Europhysics Conference on High-Energy Physics (HEP 2001), Budapest, Hungary, 12-18 Jul 2001, hep-ph/0110026;
    S. Mishima, Phys. Lett. B **521**, 252 (2001), hep-ph/0107206.

21. BELLE Collaboration, K. Abe *et al.,* KEK-PREPRINT-2001-74, BELLE-CONF-0113 (2001).

22. CLEO Collaboration, R. A. Briere *et al.,* Phys. Rev. Lett. **86**, 3718 (2001), hep-ex/0101032.

23. CLEO Collboration, S. J. Richichi *et al.,* Phys. Rev. Lett. **85**, 520 (2000), hep-ex/9912059.

24. P. Ko, Talk given at 4th International Workshop on Particle Physics Phenomenology, Kaohsiung, Taiwan, China, 18-21 Jun 1998, hep-ph/9810300.

25. H. H. Asatrian, H. M. Asatrian, D. Wyler, Phys. Lett. B **470**, 223 (1999), hep-ph/9905412.

26. A. Ali *et al.,*Phys. Rev. D **61**, 074024 (2000), hep-ph/9910221.